Polym. Bull. (2010) 64:67–79
DOI 10.1007/s00289-009-0140-1

Thermodegradative and morphological behavior of composites of HDPE with surface-treated hydroxyapatite

Carmen Albano · L. Cataño · R. Perera · A. Karam · G. González

Received: 3 February 2009 / Revised: 9 May 2009 / Accepted: 14 July 2009 /
Published online: 25 July 2009

Abstract In the present work, the thermodegradative and morphological behavior of composites of high-density polyethylene and surface-treated hydroxyapatite (HDPE/HA) were studied. Composites were prepared with HDPE, 30 wt% of HA and 2 phr of an ethylene–acrylic acid copolymer (20 wt% of acrylic acid) (EAA) and melt-blended in an internal mixer at 160 °C and 50 rpm. Two sets of composites filled with different surface-treated hydroxyapatite (STHA) were prepared: one HA sample was pretreated with ethylene–acrylic acid copolymer ($STHA_1$) and the other one with acrylic acid ($STHA_2$). Thermogravimetric analyses were carried out to evaluate the thermal stability of the composites. The activation energies (Ea) were determined using a numerical method based on the Invariant Kinetic Parameters (IKP). The thermal decomposition of the HDPE/HA composites showed an Ea value of 330 kJ/mol. On the other hand, HDPE/HA/EAA and HDPE/$STHA_1$ composites showed a sudden decrease in Ea (272 and 270 kJ/mol, respectively). The HDPE/$STHA_2$ composite exhibited an Ea value of 313 kJ/mol, slightly lower than that of the HDPE/HA composite. Additionally, with the presence of EAA

C. Albano · L. Cataño · A. Karam
Laboratorio de Polímeros, Centro de Química,
Instituto Venezolano de Investigaciones Científicas, Caracas, Venezuela

C. Albano (✉)
Universidad Central de Venezuela, Facultad de Ingeniería,
Escuela de Ingeniería Química, Caracas, Venezuela
e-mail: calbano@ivic.ve; carmen.albano@ucv.ve

R. Perera (✉)
Departamento de Mecánica, Universidad Simón Bolívar,
Valle de Sartenejas, Caracas, Venezuela
e-mail: rperera@usb.ve

G. González
Departamento de Ingeniería, Instituto Venezolano de Investigaciones Científicas,
Caracas, Venezuela

copolymer and acrylic acid in the composites, the nucleation and nucleus growth kinetic-model probabilities decreased compared to those of the HDPE/HA composite. However, there was an increase in the probability of the reaction order of the model. This behavior could be attributed to the morphology of the composites and to the addition of a less thermally stable component, i.e. EAA copolymer and acrylic acid. On the other hand, due to the interaction polymer/surface-treated filler, an increase in the Young Modulus and the tensile strength was observed.

Keywords Degradative behavior · Morphological behavior · Invariant kinetic parameters (IKP) · HDPE/HA · Mechanical behavior · Composites

Introduction

Polyolefins are materials with a wide range of applications due to their properties, versatility and low cost. From the toy industry to complex engineering applications, these materials have exhibited an outstanding performance. However, there are many areas in which polyolefins are limited due to their mechanical properties. In order to improve their performance, inorganic fillers are being used to reinforce polyolefins. For instance, hydroxyapatite (HA)-filled high-density polyethylene (HDPE) not only has shown improved mechanical properties but has also revealed a potentially increasing performance as a biomaterial because of its resemblance with bone physical properties [1–3].

Some works have reported the use of unsaturated monomers such as acrylic acid (AA) in order to be grafted onto PE, promoting interfacial adhesion when HA is employed as filler [4–6]. Wang and Bonfield [4] reported an increase in ductility and tensile strength of AA-grafted HDPE composites filled with HA. Additionally, Huang et al. [6] promoted HA biomineralization in the PE when grafted with AA, improving the mechanical properties of the composite as well.

On the other hand, modeling the thermal decomposition of a composite allows us to study the thermal stability of the HDPE/HA composite in order to elucidate how the ethylene–acrylic acid (EAA) copolymer and AA are interacting with it.

Therefore, in the present work, the activation energy (Ea) of composites of HDPE containing 30 wt% of HA was evaluated with and without the addition of an EAA or of AA. The possible decomposition mechanisms and tensile properties were also determined.

Experimental

A commercial HDPE supplied by Polinter (MFR = 5 dg/min, $\rho = 0.94$ g/cm^3) was used as the polymeric matrix. An ethylene–acrylic acid random block copolymer (EAA) containing 20 wt% of acrylic acid and acrylic acid (AA) were supplied by Sigma-Aldrich. Calcium hydroxide was purchased from Mallinckrodt and ammonium phosphate was supplied by Fischer Scientific.

Hydroxyapatite granules were prepared trough a precipitation reaction between calcium hydroxide, $Ca(OH)_2$, and ammonium phosphate $(NH_4)_2HPO_4$ solutions, according to a method described in the literature [7]. The resultant solutions were centrifuged and washed with deionized water until neutral pH to finally being vacuum dried at 65 °C for 48 h. Morphological studies of the synthesized HA were carried out using a scanning electron microscope (SEM), Hitachi FE-5400. The surface of the HA was coated with gold by the ionic deposition method. Figure 1 shows a micrograph of the synthesized HA.

Surface treatment with EAA copolymer

Hydroxyapatite surface treatment was carried out in solution, where 1 g of EAA copolymer was dissolved during 20 min in 200 ml of decalin heated at 130 °C under continuous stirring. After that period, the temperature was lowered to 80 °C. Triethanolamine (TEA) was then added to the solution (1 ml) and left apart for about 10 more minutes. The HA powder (about 15 g) was incorporated to that final solution and the stirring was kept for another 20 min. The solution was washed with ethanol and vacuum-filtered. The slurry was then vacuum-dried at 80 °C for 48 h in order to remove the solvent. The resultant powder was prepared for compounding.

AA surface treatment

Initial conditions were similar to the above mentioned procedure. First, 0.5 mL of AA were added to decalin at 80 °C and kept for 10 min. After that, 1 ml of TEA was incorporated into the solution. The following steps were the same as those described before.

Composites were prepared in a Rheomix internal mixer. High-density polyethylene was added to the mixing chamber at 160 °C and at a screw rate of 50 rpm. Subsequently, 20 phr of EAA was added to the HDPE matrix in the HDPE/HA/EAA composite. Untreated or treated HA addition at the corresponding amounts followed, in order to have a concentration of 30 wt%. Then, the screw rate was

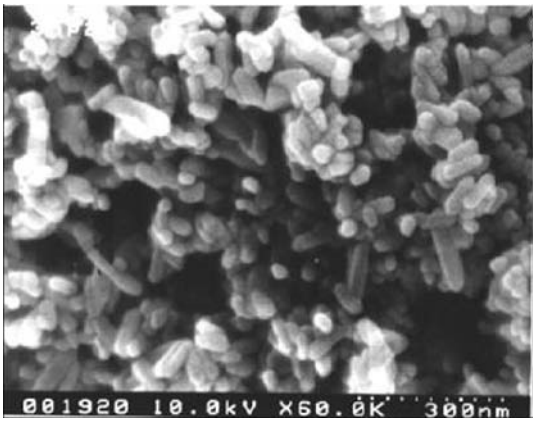

Fig. 1 SEM micrograph of the synthesized HA

increased to 90 rpm for 8 more min. Material codes for all the prepared samples can be seen in Table 1.

Mechanical properties were determined in an Instron Universal Testing Machine (model 4204) at 50 mm/min. The specimens were cut out from compression-molded sheets and their dimensions followed ASTM-638 standard procedure. Each tensile parameter reported represents an average of at least seven samples tested under identical conditions.

Transmission electron microscopy (TEM) analyses were performed using a Phillips CM10 microscope. Samples were prepared by ultramicrotomy without any further conditioning.

Thermograms were obtained by thermogravimetric analysis (TGA) using a Mettler-Toledo TGA/STDA851^e thermal analyzer under the following conditions: samples of 5–6 mg each were heated up to a temperature of 800 K under nitrogen atmosphere at various heating rates ($\beta_i = 5$, 10, 15 and 20 K/min). The thermal kinetic parameters were determined by means of the Invariant Kinetic Parameters (IKP) method [8–13].

Invariant Kinetic Parameters method: description

The IKP method is based on the decomposition rate ($d\alpha/dt$), which is equal to the following equation:

$$\frac{d\alpha}{dt} = k \times f(\alpha) \tag{1}$$

where α is the degree of conversion and $k = A \times \exp(-E/RT)$ according to the Arrhenius law.

Eighteen apparent activation energies (E_{iv}) and pre-exponential factors (A_{iv}) are determined employing the Coats–Redfern method [14]. The IKP method is based on the principle of the compensation effect quite well reviewed in the literature. For each function $f_j(\alpha)$ proposed by the method, $log(A_j)$ versus E_j was plotted. If a compensation effect is observed, then a linear relationship is seen for each heating rate β_v, which is defined by the following expression:

Table 1 Material codes

Materials	Code
High-density polyethylene with 30 wt% of untreated hydroxyapatite	HDPE/HA
High-density polyethylene with 30 wt% of hydroxyapatite and 2 phr of ethylene–acrylic acid copolymer containing 20 wt% of acrylic acid.	HDPE/HA/EAA
High-density polyethylene with 30 wt% of EAA-copolymer surface-treated hydroxyapatite	HDPE/STHA$_1$
High-density polyethylene with 30 wt% of AA-surface-treated hydroxyapatite	HDPE/STHA$_2$

$$\log A_{iv} = B_v + l_v E_{jv} \tag{2}$$

where A_{iv} and E_{jv} are the apparent pre-exponential factor and the activation energy, respectively, calculated using a function $f_j(\alpha)$ at β_v. $f_j(\alpha)$ is given in Table 2 for each kinetic model. Also the values of the integral conversion function, $g_j(\alpha)$, are shown there [9].

Inappropriate assigning of the kinetic model function results in the distortion of the kinetic parameters and in the false or superficial classification of the compensation effect.

The values B_v and l_v are calculated from the intercept and the slope of the straight lines obtained by Eq. 2. Lesnikovich and Levchik [15, 16] and Levchik et al. [17] discussed the significance of these values and demonstrated the following relationships:

$$B_v = \log(k_v) \tag{3}$$

$$l_v = (2.3RT_v)^{-1} \tag{4}$$

where k_v is the rate constant of the system at the temperature T_v; these two parameters are characteristics of the experimental conditions.

The curves $\log(k_v)$ versus $1/T_v$ are plotted in order to calculate the intercept and slope of this equation:

Table 2 Degradation functions used in the IKP method [8]

Kinetic model	$f_j(\alpha)$	$g_j(\alpha)$	Observations
A	$\frac{1}{n}(1-\alpha)(-\ln(1-\alpha))^{1-n}$	$(-\ln(1-\alpha))^n$	S1-n = 1/4
			S2-n = 1/3
			S3-n = 1/2
			S4-n = 2/3
B	$(1-\alpha)^n$	$1-(1-\alpha)$	S6 Plane symmetry
		$2[1-(1-\alpha)^{1/2}]$	S7 Cylindrical symmetry
		$3[1-(1-\alpha)^{1/3}]$	S8 Spherical symmetry
C	$1/2\alpha^{-1}$	α^2	S9 Plane symmetry
	$(-\ln(1-\alpha))^{-1}$	$(1-\alpha)\ln(1-\alpha)+\alpha$	S10 Cylindrical symmetry
	$3/2[(1-\alpha)^{-1/3}-1]^{-1}$	$1-2/3\alpha-(1-\alpha)^{2/3}$	S11 Spherical symmetry
	$3/2(1-\alpha)^{1/3}[(1-\alpha)^{-1/3}-1]^{-1}$	$[(1-\alpha)^{1/3}-1]^2$	S18 Jander's type
D	$(1/n)\alpha^{1-n}$	$\alpha^n (0<n<2)$	S12-n = 1/4
			S13-n = 1/3
			S14-n = 1/2
			S17-n = 3/2
E	$(1-\alpha)$	$-\ln(1-\alpha)$	S5-n = 1
	$(1/n)(1-\alpha)^{1-n}$	$1-(1-\alpha)^{1/2}$	S15-n = 1/2
		$1-(1-\alpha)^{1/3}$	S16-n = 1/3

A Nucleation and nucleus growth, *B* phase boundary reaction, *C* diffusion, *D* potential law, *E* reaction order

$$\log(k_v) = \log(A_{inv}) - E_{inv}/2.3RT_v \tag{5}$$

which finally result in the values of the invariant activation energy (E_{inv}) and the pre-exponential factor (A_{inv}) of the evaluated sample.

Once the invariant kinetic parameters (A_{inv} and E_{inv}) are obtained, the probability of occurrence of the mechanisms shown in Table 2 is determined.

To do so, a statistical treatment [18] is carried out calculating the squared-minima for each function $f_j(\alpha)$ at each heating rate β_v, through the following expression:

$$(n-1)S_{jv}^2 = \sum_{i=1}^{i=n} \left| \left(\frac{d\alpha}{dT}\right)_{iv} - \frac{A_{inv}}{\beta_v} \exp\left(-\frac{E_{inv}}{RT_{iv}}\right) f_j(\alpha_{iv}) \right|^2 \tag{6}$$

The most probable function is chosen through the minimum average value $\overline{S_j}$ defined by the following expression:

$$\bar{S}_j = \frac{1}{p} \sum_{v=1}^{v=p} S_{jv} \tag{7}$$

where p is the number of heating rates.

The probability associated to each $f_j(\alpha)$ function is calculated using the equation:

$$F_j = \frac{\bar{S}_j^2}{\bar{S}_{\min}^2} \tag{8}$$

where $\overline{S}_{\min}^2$ is the minimum average of the residual dispersion. This relationship obeys a distribution F which equals:

$$q(F_j) = \frac{\Gamma(v) \quad F_j^{(v/2)-1}}{\Gamma^2(v/2)(1+F_j)^v} \tag{9}$$

where the number of degrees of freedom (n) for every dispersion equals the number of heating rates used (p) and Γ is the gamma function.

The probabilities of the jth function are computed on the assumption that the experimental data with L kinetic functions are described by a complete and independent system of events:

$$\sum_{j=1}^{j=L} P_j = 1 \tag{10}$$

In this way, P_j can be obtained:

$$P_j = \frac{q(F_j)}{\sum_{j=1}^{j=L} q(F_j)} \tag{11}$$

with the employed L kinetic functions (Table 2).

The thermal behavior of a material depends on processes occurring in both the condensed and gas phases and on the processes of heat and mass transfer. These processes strongly depend on the mode of degradation on the material [19] (Fig. 2).

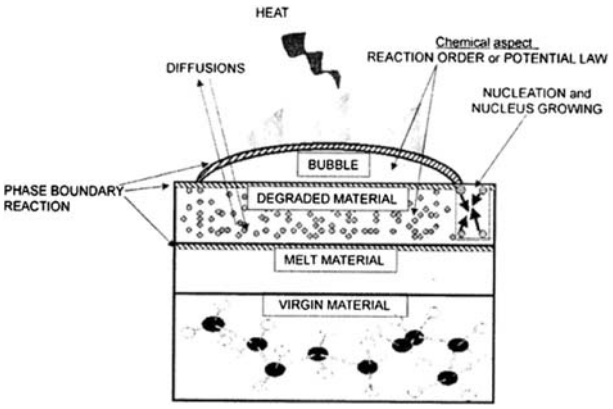

Fig. 2 Thermal degradation: different mechanisms [19]

Therefore, modeling the thermal degradation of a material is an important task for the understanding of the mechanisms occurring in the condensed phase and the degradation mode of the material can thus be deduced.

Results and discussion

To study the thermal stability of the composites, the IKP method was used [8–13]. Table 3 shows that those composites containing AA units display a decrease in the E_{inv} values. This fact is attributed to the lower activation energy of pure AA (170 kJ/mol), as a consequence of the presence of carboxylic groups in its structure. Thus, a decrease in the thermal stability of the composites is produced. The same tendency is displayed by the composite containing only pure AA.

In general terms, Figs. 3, 4, 5 and 6 display that all composites unfold increased probabilities for mechanisms given in Table 2, corresponding to the "reaction order" kinetic model (S15 and S16), and mechanisms corresponding to the "nucleation and nucleus growth" kinetic model (S1, S2 and S3).

The variations observed, specifically in mechanisms S1, S2, S15 and S16, are associated to diverse factors such as the formation of gases, the chemical nature of the components of the composites, the chemical reactions that are produced and to the presence of agglomerates and the dispersion of the HA in the HDPE matrix. This

Table 3 Activation energy determined by IKP

Simple	Ea (kJ/mol)
HDPE/HA	330.2
HDPE/HA/EAA	271.8
HDPE/STHA$_1$	270.2
HDPE/STHA$_2$	312.6

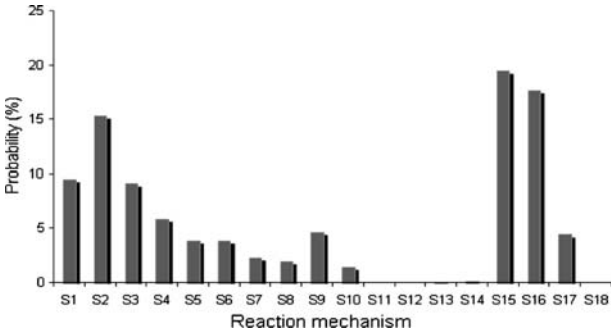

Fig. 3 Probabilities of the HDPE/HA composite evaluated by IKP

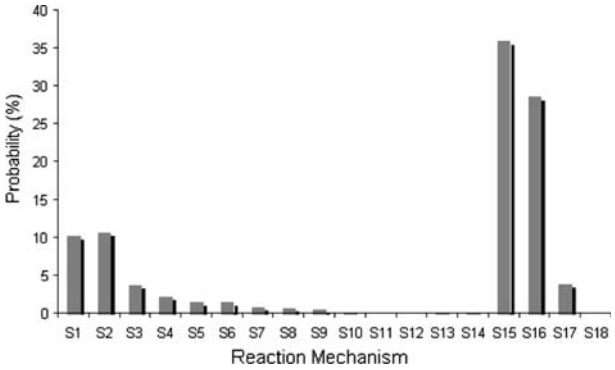

Fig. 4 Probabilities of the HDPE/HA/EAA composite evaluated by IKP

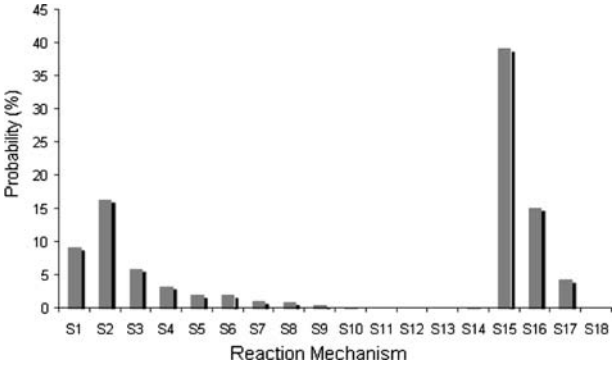

Fig. 5 Probabilities of the HDPE/$STHA_1$ composite evaluated by IKP

is a consequence of the fact that the degradation of a polymeric material often cannot be represented by a single function, but by a set of functions because of the different processes which can occur during the degradation of the material in series or in parallel.

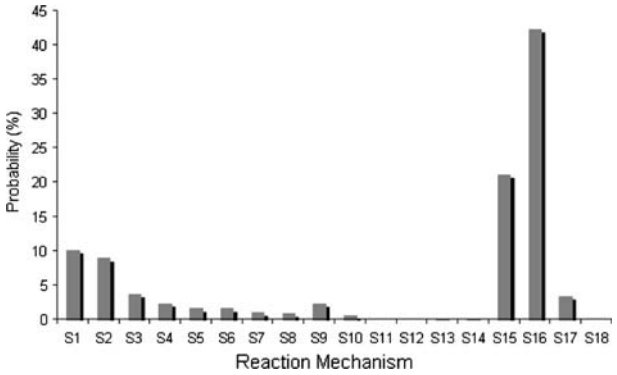

Fig. 6 Probabilities of the HDPE/STHA$_2$ composite evaluated by IKP

Figure 4 shows that the addition of the EAA copolymer to the HDPE/HA composite increases in 50% the probability of occurrence of the reaction mechanisms corresponding to the kinetic models S15 and S16, being this increment higher in those composites treated with triethanolamine (Figs. 5 and 6).

The decomposition mechanisms depend on the reactivity of the carboxylic group in AA. Hence, it can be inferred that carboxylic groups are responsible for the increased probability of mechanisms corresponding to the "reaction order" kinetic model (S15, S16), which implies a high reactivity of this group in the HDPE/HA/EAA, HDPE/STHA$_1$ and HDPE/STHA$_2$ composites.

When treatments with triethanolamine were performed, in HDPE/STHA$_1$ and HDPE/STHA$_2$ composites, the probability of occurrence of mechanisms S15 and S16 is significantly increased, when compared to that corresponding to HDPE/HA/EAA. On the other hand, the HDPE/HA composite displays a higher probability towards the kinetic mechanisms corresponding to kinetic models "nucleation and nucleus growth" (S1, S2, S3).

The probable degradation functions $f_j(\alpha)$ are presented in Fig. 7. The equation is:

$$f(\alpha) = \sum_{j=1}^{18} P_j(\%) f_j(\alpha_j) \tag{12}$$

Composites HDPE/HA/EAA and HDPE/STHA$_1$, which display the lower values of E_{inv}, unfold a slight maximum at conversions of 20 and 30%. This could indicate that the mechanisms are accelerated as soon as the degradation initial stages are over, resulting in low thermal stability composites. On the contrary, the behavior of the HDPE/HA composite exhibits a plateau at the initial stages of the degradation, which could imply that at conversions of up to 40%, the decomposition mechanisms involved remain approximately constant. The HDPE/STHA$_2$ composite displays an initial decrease at low conversions. It is possible that the AA that did not react in the pretreatment stage, is the responsible for the decreased values of the kinetic functions associated to the initial stages of decomposition.

The morphology of the composites has a strong influence in the probability of occurrence of the different decomposition mechanisms. In the HDPE/HA

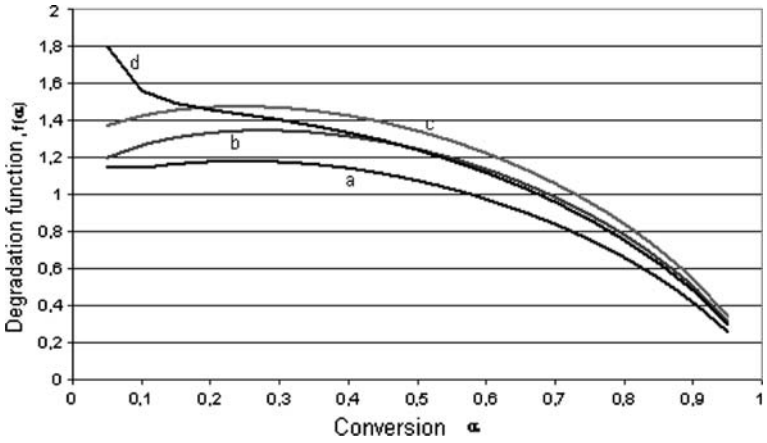

Fig. 7 Degradation function versus degree of conversion. *a* HDPE/HA, *b* HDPE/STHA$_1$, *c* HDPE/HA/EAA, *d* HDPE/STHA$_2$

composite, the morphology presented in Fig. 8 displays some agglomerates. Hence, it is possible that some radical cluster could be formed at the interface, which could initiate the decomposition process through the "nucleation and nucleus growth" kinetic models (S1, S2 and S3). This fact can be confirmed through the probability values of this composite, when compared to those of the other composites.

On the contrary, HDPE/HA/EAA, HDPE/STHA$_1$ and HDPE/STHA$_2$ composites display a better filler dispersion, which could imply a higher polymer–filler interaction (Figs. 8, 9, 10). This can be seen in Figs. 9 and 10, where the distribution of HA is more homogeneous and the nanoparticles are well dispersed in the polymer matrix, specially in the composites where HA was previously surface treated HDPE/

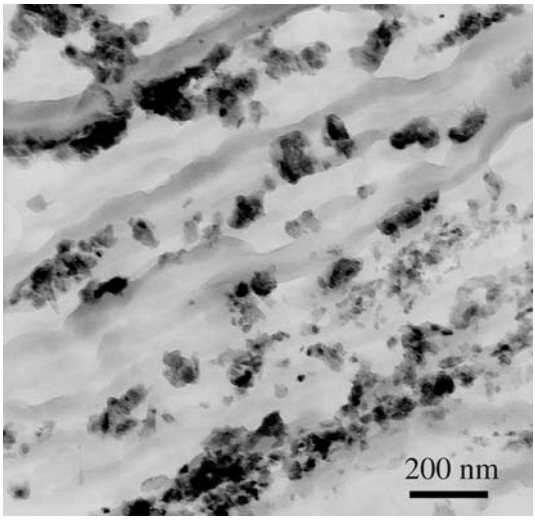

Fig. 8 TEM micrograph of HDPE/HA composite

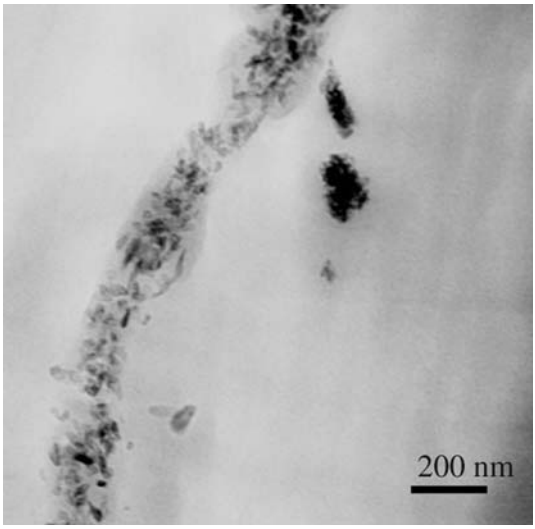

Fig. 9 TEM micrograph of HDPE/HA/EAA composite

$STHA_1$ and HDPE/$STHA_2$ materials (Fig. 10a, b), implying that the groups present at the interface significantly improved the interation with the matrix.

From Fig. 2, the degradation process in the polymer starts in the melt, where a gas phase is formed, which, in addition to the radicals produced brings about the mechanism of "nucleation and nucleus growth". This process can be altered when the temperature increases and the carbonization of the polymer is produced. The polymer contains macropores, which give way to the diffusion process corresponding to the S9 and S10 kinetic models. But, due to the fact that this process is slow, the associated probabilities are low. These probabilities decrease in composites containing AA due to the reactivity of the carboxylic groups with the aqueous phase

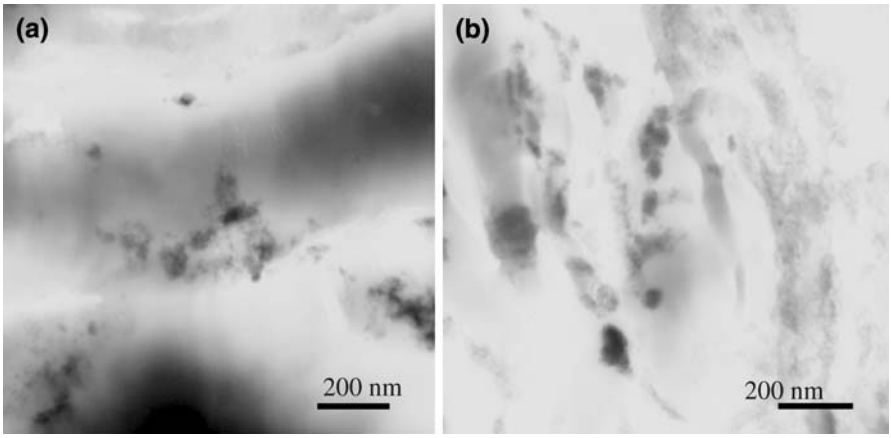

Fig. 10 TEM micrographs of **a** HDPE/STHA1, and **b** HDPE/STHA2 composites

Table 4 Mechanical properties of the composites

Samples	Young's modulus (MPa)	Tensile strength (MPa)	Elongation at break (%)
HDPE/HA	455 ± 21	19.49 ± 1.05	8.8 ± 1.0
HDPE/HA/EAA	520 ± 12	21.17 ± 0.45	9.4 ± 0.7
HDPE/STHA$_1$	556 ± 1	22.47 ± 0.57	10.6 ± 1.0
HDPE/STHA$_2$	558 ± 12	21.40 ± 0.61	11.4 ± 0.5

formed in the melt, thus favoring the mechanisms corresponding to the "reaction order" kinetic model (S15 and S16).

The different treatments improved the filler dispersion (Figs. 8, 9, 10), thus improving the mechanical behavior of the composites. This is reflected in their Young's modulus values and tensile strength. A higher increase was obtained when the HA was pretreated with triethanolamine (Table 4). However, no significant changes were found in the values of elongation at break, despite the better dispersion of the filler. This fact can be attributed to the absence of strong chemical interactions between the phases.

Conclusions

- The IKP was useful in determining the more probable reaction mechanisms in the degradation process of the studied composites. The HDPE/HA composite displayed increased probabilities for mechanisms S1, S2, S3, and S15, S16, corresponding to "nucleation and nucleus growth" and "reaction order" kinetic models, respectively.
- On the contrary, the HDPE/HA/EAA, HDPE/STHA$_1$ and HDPE/STHA$_2$ composites displayed the higher probabilities for mechanisms S15 and S16, decreasing those for mechanisms S1, S2 and S3.
- The morphology of the composites significantly influenced the probabilities of occurrence of the different decomposition mechanisms proposed in the IKP kinetic model.
- The Young's modulus and tensile strength values increased due to increased polymer-filler interactions, specially in those composites where the HA was treated with triethanolamine.

References

1. Wang M, Porter D, Bonfield W (1994) Processing, characterisation, and evaluation of hydroxyapatite reinforced polyethylene composites. Br Ceram Trans 93:91–95
2. Tanner KE, Downes RN, Bonfield W (1994) Clinical applications of hydroxyapatite reinforced materials. Br Ceram Trans 93:104–107

3. Wang M, Berry C, Braden M, Bonfield W (1998) Young's and shear moduli of ceramic particle filled polyethylene. J Mater Sci Mater Med 9:621–624
4. Deb S, Wang M, Tanner KE, Bonfield W (1996) Hydroxyapatite–polyethylene composites: effect of grafting and surface treatment of hydroxyapatite. J Mater Sci Mater Med 7:191–193
5. Wang M, Bonfield W (2001) Chemically coupled hydroxyapatite–polyethylene composites: structure and properties. Biomaterials 22:1311–1320
6. Huang S, Zhou K, Zhu W, Huang B, Li Z (2006) Effects of in situ biomineralization on microstructural and mechanical properties of hydroxyapatite/polyethylene composites. J Appl Polym Sci 101:1842–1847
7. Spadavecchia U, González G (2007) Obtencion de hidroxiapatita nanometrica para aplicaciones medicas. Rev Fac Ing UCV 22:37–44
8. Bourbigot S, Delobel R, Le Bras M, Normand D (1993) Comparative study of the integral TG methods used in the invariant kinetic parameter method. Application to the fire-retardant polypropylene. J Chim Phys 90:1909–1928
9. Budrugeac P, Segal E, Perez-Maqueda LA, Criado JM (2004) The use of the IKP method for discerning the kinetic parameters and the conversion function of the thermal dehydroclorination of PVC from non-isothermal data. Polym Degrad Stab 84:311–320
10. Budrugeac P (2005) Some methodological problems concerning the kinetic analysis of non-isothermal data for thermal and thermo-oxidative degradation of polymers and polymeric materials. Polym Degrad Stab 89:265–273
11. Cataño L, Albano C, Karam A, Perera R, Silva P (2007) Thermal stability evaluation of PA6/LLDPE/SEBS-g-DEM blends. Macromol Symp 257:147–157
12. Budrugeac P, Musat V, Segal E (2007) Non-isothermal kinetic study ofthe decomposition of ZnAcetate-based sol-gel precursor. II. The application of IKP method. J Thermal Anal 88:699–702
13. Rotaru A, Bratulescu G, Rotaru P (2009) Thermal analysis of azoic dyes: Part I. Non-isothermal decomposition kinetics of [4-(4-chlorobenzyloxy)-3-methylphenyl](*p*-tolyl)diazene in dynamic air atmosphere. Thermochim Acta 489(6):3–69
14. Coats AW, Redfern JP (1964) Kinetic parameters from thermogravimetric data. Nature 201:68–69
15. Lesnikovich AJ, Levchik SV (1983) A method of finding invariant values of kinetic parameters. J Thermal Anal 27:89–93
16. Lesnikovich AJ, Levchik SV (1985) Isoparametric kinetic relations for chemical transformations in condensed substances (analytical survey). II. Reactions involving the participation of solid substances. J Thermal Anal 30:677–702
17. Levchik SV, Levchik GF, Lesnikovich AJ (1985) Analysis and development of effective invariant kinetic parameters finding method based on the non-isothermal data. Thermochim Acta 92:157–160
18. Miller I, Freund J (2004) Probability and statistics for engineers, 7th edn. Prentice Hall, USA
19. Almeras X, Dabrowski F, Le Bras M, Delobel R, Bourbigot S, Marosi G, Anna P (2002) Using polyamide 6 as charring agent in intumescent polypropylene formulations II. Thermal degradation. Polym Degrad Stab 77:315–323